Neuronal BST2: A Pruritic Mediator alongside Protease-Activated Receptor 2 in the IL-27−Driven Itch Pathway

Yanqing Li[1], Weiwei Chen[1], Xingyun Zhu[1], Huiyuan Mei[1], Martin Steinhoff[2,3,4,5,6,7], Joerg Buddenkotte[2,3,4], Jinhai Wang[1], Wenhao Zhang[1], Zhenghui Li[8], Xiaolong Dai[1], Chunxu Shan[9], Jiafu Wang[9,10] and Jianghui Meng[9,10]

Chronic itch is a common and complex symptom often associated with skin diseases such as atopic dermatitis (AD). Although IL-27 is linked to AD, its role and clinical significance in itch remain undefined. We sought to investigate IL-27 function in itch using tissue-specific transgenic mice, various itch models, behavior scoring, RNA sequencing, and cytokine/kinase array. Our findings show that IL-27 receptors were overexpressed in human AD skin. Intradermal IL-27 injection failed to directly induce itch in mice but upregulated skin protease-activated receptor 2 (PAR2) transcripts, a key factor in itch and AD. IL-27 activated human keratinocytes, increasing *PAR2* transcription and activity. Coinjection of SLIGRL (PAR2 agonist) and IL-27 in mice heightened PAR2-mediated itch. In addition, IL-27 boosted *BST2* transcription in sensory neurons and keratinocytes. BST2 was upregulated in AD skin, and its injection in mice induced itch-like response. BST2 colocalized with sensory nerve branches in AD skin from both human and murine models. Sensory neurons released BST2, and mice with sensory neuron−specific BST2 knockout displayed reduced itch responses. Overall, this study provides evidence that skin IL-27/PAR2 and neuronal IL-27/BST2 axes are implicated in cutaneous inflammation and pruritus. The discovery of neuronal BST2 in pruritus shed light on BST2 in the itch cascade.

INTRODUCTION

Chronic itch is a common and debilitating symptom of many systemic and cutaneous disorders, including atopic dermatitis (AD) and prurigo nodularis, for example (Steinhoff et al, 2018). Pruritic skin conditions are characterized by skin lesions and dysregulated intercellular communication, leading to overactivation of peripheral itch pathways and induction of the pathological itch/scratch cycle (Steinhoff et al, 2022). Despite the prevalence and impact of chronic itch, the Food and Drug Administration has yet to approve specific or targeted anti-itch agents (Wang and Kim, 2020).

Cytokines play an essential role in neuroimmune circuits and pruritus (Steinhoff et al, 2022; Trier and Kim, 2018). Cytokines (eg, IL-4, IL-13, IL-31) and their Jak/signal transducer and activator of transcription (STAT)−mediated signaling pathways (eg, Jak1, Jak2) have demonstrated the benefit of cytokine inhibition for treatment of pruritic and inflammatory skin diseases (Sutaria et al, 2022). IL-27 is a member of the IL-6/IL-12 cytokine family, a group that also includes IL-31, a critical mediator in itch generation and cutaneous AD−associated inflammation (Cevikbas et al, 2014; Müller et al, 2019). Functional IL-27 is composed of 2 subunits: IL-27p28 (also known as IL-27A or IL-30) and EBI3. These 2 subunits come together to form the functional IL-27 cytokine. In the skin, IL-27 is released by epidermal keratinocytes and antigen-presenting cells such as macrophages and dendritic cells. Cutaneous IL-27 regulates the activity of T helper (Th) cells, inhibiting the development of Th17 cells, downregulating Th1-mediating inflammation, and modulating Th2 development and cytokine release (Yoshimoto et al, 2007). Accordingly, IL-27 has been suggested as a potential therapeutic molecule for the treatment of Th2 cell−mediated allergic conditions (Yoshimoto et al, 2007). However, IL-27 also activates keratinocytes and promotes keratinocyte-derived inflammation, thus hampering its therapeutic utility as a T-cell modulator. Specifically, in keratinocytes, IL-27 stimulates STAT1 and STAT3 pathways, promotes major histocompatibility complex class I

[1]School of Life Sciences, Henan University, Henan, China; [2]Department of Dermatology and Venereology, Hamad Medical Corporation, Doha, Qatar; [3]Translational Research Institute, Academic Health System, Hamad Medical Corporation, Doha, Qatar; [4]Dermatology Institute, Academic Health System, Hamad Medical Corporation, Doha, Qatar; [5]Department of Dermatology, Weill Cornell Medicine-Qatar, Doha, Qatar; [6]College of Medicine, Qatar University, Doha, Qatar; [7]Israel Englander Department of Dermatology, Weill Cornell Medicine, New York, New York, USA; [8]Department of Neurosurgery, The Third Affiliated Hospital of Zhengzhou University, Zhengzhou, China; and [9]School of Biotechnology, Faculty of Science and Health, Dublin City University, Dublin, Ireland

[10]These authors contributed equally as senior authors.

Correspondence: Jianghui Meng, School of Biotechnology, Faculty of Science and Health, Dublin City University, Glasnevin Avenue, Dublin 9, Ireland. E-mail: Jianghui.meng@dcu.ie

ARTICLE IN PRESS

Y Li et al.
Neuronal BST2: Pruritic Mediator in IL-27−Driven Itch

expression, enhances CXCL10 production, and sensitizes TNF-α signaling (Wittmann et al, 2009).

The biological effects of IL-27 are mediated by a cell-surface receptor complex comprised of IL-27RA (IL-27 receptor α chain, also known as WSX-1 or TCCR) and GP130, a common receptor subunit for IL-6 family cytokines (Hunter and Kastelein, 2012). These receptor subunits are expressed in a variety of cells, including mast cells, monocytes, and keratinocytes (Hunter and Kastelein, 2012; Pflanz et al, 2004); however, their distribution in normal and diseased human skin is still unclear. Although GP130 has been detected in peripheral neurons, whether IL-27 could directly activate sensory neurons remained unexplored. We sought to address these gaps in knowledge and assess the importance of IL-27 signaling in peripheral itch transduction.

Mounting evidence implicates IL-27 in AD and other chronic, immune-related conditions such as rheumatoid arthritis, multiple sclerosis, and pain. IL-27 may play distinct roles in each of these conditions and represent both a proinflammatory and anti-inflammatory cytokine (Wittmann et al, 2012). IL-27 is found highly upregulated in chronic AD lesions, with IL-27 levels being linked to lesional progression (Wittmann et al, 2009). However, the importance of IL-27 and related signaling in lesion-associated itch was unexplored.

BST2, also known as tetherin or CD317, is a lipid raft−associated type II transmembrane glycoprotein protein primarily induced by type I IFN signaling. BST2 acts as an antiviral factor and regulates host immune responses (Tiwari et al, 2019), but its function is versatile and largely undermined depending on the specific cell type. BST2 is an inducible gene product under the control of inflammatory signals (Cao et al, 2009) and can be induced by IL-27 in human monocytes and T cells (Guzzo et al, 2012). BST2 has also been implicated in immunomodulation in tumorigenesis (Mahauad-Fernandez et al, 2014). Although BST2 is known to be involved in the growth and development of B cells, plays an important role in antiviral response, and acts as a non−major histocompatibility complex class I−type ligand for a member of the ILT receptor family (Brown et al, 2004), so far, its role in dermatological diseases is not clear.

In this study, we aim to delineate the role of IL-27 signaling in pruritic skin conditions, in particular, in chronic itch of AD. The importance of IL-27 signalling and the possible involvement of BST2 as well as the linkage with other itch modulators in peripheral itch transduction will be investigated. Our results strongly suggest a role of IL-27 and BST2 in cytokine-mediated pruritus and neuroimmune circuits in AD.

RESULTS

IL-27 does not induce itching in mice but it enhances protease-activated receptor 2 transcription and activity. Coinjecting SLIGRL or trypsin and IL-27 intensified the itch response in the cheek model

Previous studies revealed that subunits of *IL27* mRNA and protein levels were correlated to chronic inflamed eczema (Wittmann et al, 2009). To understand the influence of IL-27 on itch generation, the impact of IL-27 on itch was assessed using an acute mice cheek model. However, intradermal injection of IL-27 (200 ng, 4 µl) did not elicit scratching behaviors versus vehicle injection (Figure 1a). Thus, IL-27 may not act as a pruritogen in mice.

To investigate the impact of IL-27 on the skin after intradermal injection, cheek skin samples that received either IL-27 or vehicle injections (4 hours) were subjected to RT-qPCR. This revealed a significant upregulation of *F2RL1*, the protease-activated receptor 2 (PAR2) transcripts (Figure 1b). This finding suggests that IL-27 might regulate this receptor linked to both itch and inflammation.

To investigate the functional alterations of PAR2 by IL-27 regulation, the transcription of *F2RL1* in cultured keratinocytes was evaluated. In this study, we treated primary human keratinocytes (phKCs) with media ± IL-27 (100 ng/ml, various time points) and measured *F2RL1* transcripts by RT-qPCR. At all tested time points, IL-27 enhanced *F2RL1* transcription (Figure 1c). This leads to the functional analysis using calcium imaging to assess whether this *F2RL1* transcriptional change would translate to enhanced PAR2 activity in cultured phKCs.

Cells were pretreated with vehicle ± IL-27 (100 ng/ml, 6 hours), loaded with a fluorescent calcium dye Fluo-4 AM, and stimulated with either the specific PAR2 agonist (SLIGRL, 10 µM) or the inactive reversed peptide (LRGILS, 10 µM) (Figure 1d). SLIGRL application successfully induced calcium transients in media ± IL-27 pretreated cells (Figure 1e). In both groups, SLIGRL-responsive cells generally displayed a rapid calcium peak (low $Time_{max}$ value) (Figure 1f). The inactive peptide, LRGILS, failed to induce comparable calcium fluctuations, even when pretreated with IL-27 (Figure 1f, right panel). Importantly, IL-27 pretreatment resulted in a slight increase in the percentage of SLIGRL-responsive phKCs (78.77 vs 81.24%) (Figure 1f, left vs middle panel). However, no significant association was found between IL-27 pretreatment and the percentage of SLIGRL-responsive cells (Figure 1g); thus, IL-27 does not increase the overall percentage of SLIGRL-responsive cells. SLIGRL-stimulated cells were then compared with respect to the area under curve metric. In this study, IL-27 pretreatment significantly increased average area under curve values relative to vehicle pretreated controls (Figure 1h), suggesting that IL-27 enhances PAR2-mediated responses in SLIGRL-responsive cells.

Next, the impact of IL-27 on the pruritogenic genesis of PAR2 was evaluated. In this study, in a mouse cheek model of itch, SLIGRL but not IL-27 elicited itch-like behaviors; however, coinjection of SLIGRL and IL-27 significantly enhanced SLIGRL-elicited itch (Figure 1i), and this is evident at multiple time points (Figure 1j).

To unravel the molecular impact of IL-27 on itch signaling, skin samples were collected from the injection site 4 hours after injection for RT-qPCR analysis of mRNA level for *Tslp*, a cytokine released by keratinocytes and can directly stimulate sensory neurons and provoke itch. Despite the absence of immediate acute scratching behavior in mice after intradermal IL-27 injection, it led to an upregulation in *Tslp* expression (Figure 1k). Furthermore, coinjection of IL-27 with SLIGRL further amplified the *Tslp* expression induced by SLIGRL (Figure 1k). Thus, TSLP might also contribute to IL-27 signaling in itch pathogenesis.

ARTICLE IN PRESS

Y Li et al.
Neuronal BST2: Pruritic Mediator in IL-27−Driven Itch
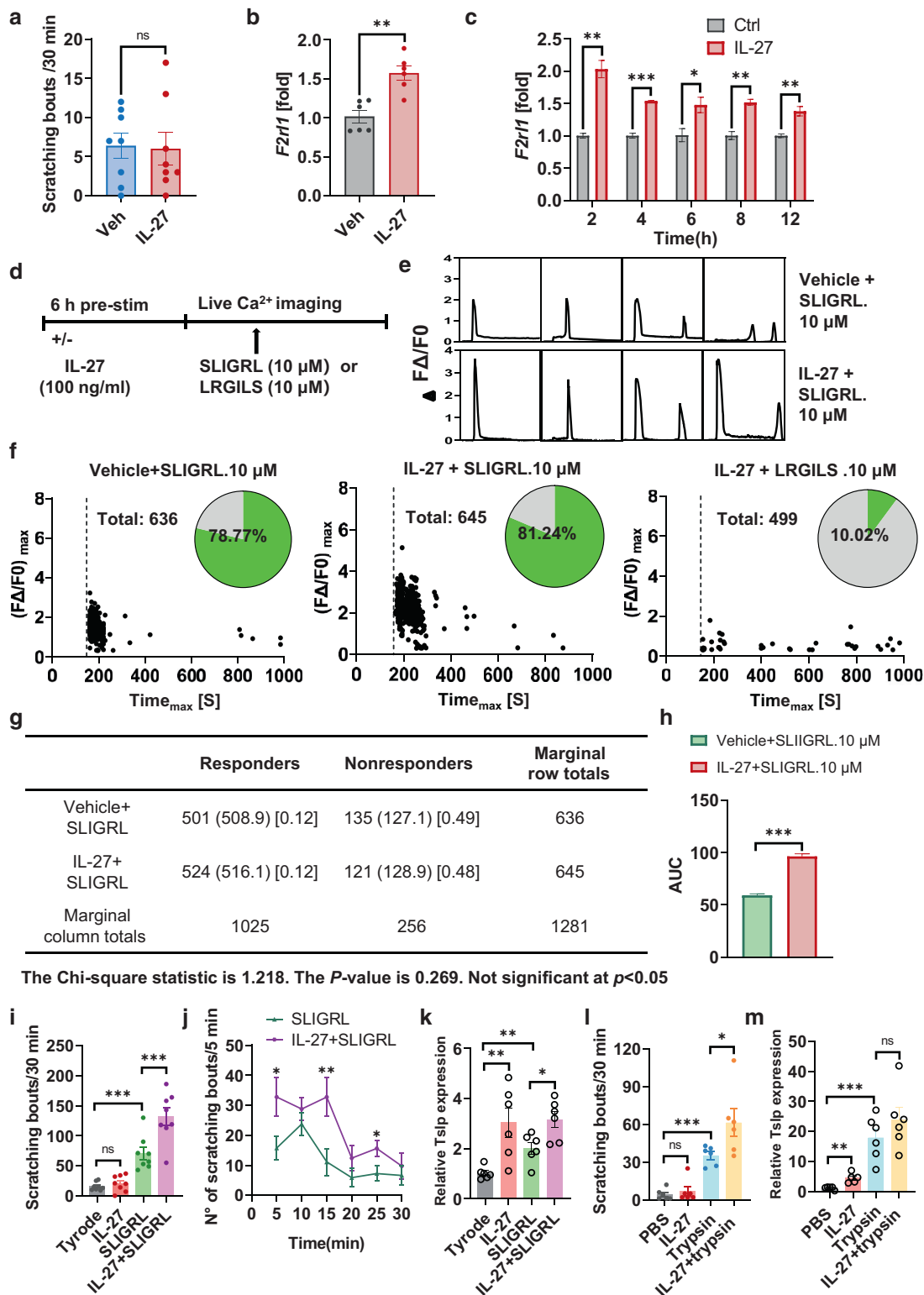
Figure 1. IL-27 potentiates PAR2 in keratinocytes. (**a**) No acute itch response was observed in mice after i.d. cheek injection of IL-27 versus vehicle (denoted as Veh). (**b, c**) IL-27 enhances F2RL1 transcription after incubation for (**b**) 4 h or (**c**) various periods. (**d**) Calcium imaging protocol in cultured phKCs for **e−h**. (**e**) Effect of IL-27 versus vehicle pretreatment on SLIGRL- or LRGILS-associated calcium mobilization. (**f**) Calcium fluctuations in vehicle or IL-27 pretreated followed by SLIGRL or LRGILS. Each dot represents a responsive phKC. Dotted lines: application of stimuli. (**g**) Charts indicating the percentage of responsive cells of **f**. (**h**) Comparison of calcium traces in AUC. (**i, j**) SLIGRL and IL-27 coinjection enhanced SLIGRL-induced scratching bouts in a (**i**) mouse cheek model and (**j**) time course response. (**k**) RT-qPCR analysis of *Tslp* mRNA levels in the mice cheek skin samples after i.d. cheek injection of IL-27, SLIGRL, or their combination. (**l**) Trypsin and IL-27 coinjection enhanced trypsin-induced scratching bouts in a mouse cheek model. (**m**) RT-qPCR analysis of *Tslp* mRNA levels in the mice cheek skin samples after i.d. cheek injection of IL-27, trypsin, or their combination. Data represent mean ± SEM (n ≥ 3 for cell-based assay

ARTICLE IN PRESS

Y Li et al.
Neuronal BST2: Pruritic Mediator in IL-27–Driven Itch

In a separate experiment, we also investigated the effect of IL-27 on trypsin-induced itch. The difference between SLIGRL and trypsin is that trypsin can activate PAR1, 2, and 4 (Cocks and Moffatt, 2000), whereas SLIGRL selectively activates PAR2. Interestingly, IL-27 also heightened the itching caused by trypsin (Figure 1l). This was associated with a trend of increase in the expression of *Tslp* over trypsin alone (Figure 1m); however, this did not reach statistical significance. In summary, our findings suggest a potential involvement of TSLP in IL-27–mediated itch signaling, highlighting an IL-27 and PAR2 interplay with TSLP in the regulation of itch-related responses.

Together, our findings demonstrate that IL-27 promotes PAR2 expression and sensitizes PAR2-mediated responses in epidermal keratinocytes, thus elevating itch responses in mice. The role of PAR2 in AD and chronic itch is well-documented (Steinhoff et al, 2003, 2000), with PAR2 regulating TSLP signaling, modulating transient potential channel function, and facilitating IL-31–induced brain natriuretic peptide synthesis, all of which are key factors in itch transduction (Cevikbas et al, 2014; Datsi et al, 2021; Dillon et al, 2004; Meng et al, 2021, 2018; Wilson et al, 2013). Thus, through PAR2 sensitization, IL-27 likely represents a key driver of pruritic cascades in AD.

IL-27 activates sensory neurons and upregulates BST2, which elicits acute itch–like behavior in mice

Although IL-27 failed to induce scratching responses in our murine model of acute itch (c.f. Figure 1a), we hypothesized that cutaneous IL-27 may still alter peripheral sensory neurons and could promote neurogenic inflammation.

To evaluate the effect of IL-27 on sensory neurons, the presence of the IL-27 receptors (IL-27RA and GP130) in cultured mouse sensory neurons was examined using immunocytochemistry, specified in this study as murine trigeminal ganglionic neurons (mTGNs), with NeuN acting as a specific marker of postmitotic neurons. This work revealed that both IL-27RA and GP130 are expressed in a small number of NeuN-positive (NeuN$^+$) cells (Figure 2a). Colocalization showed that IL-27RA$^+$ neurons represent a subpopulation of GP130$^+$ neurons, with each representing ∼4.7 and ∼6.5% of total neurons, respectively (Figure 2b).

To assess whether cutaneous IL-27 could directly activate peripheral sensory neurons, we examined the effect of IL-27 on calcium fluctuations in cultured mTGNs. Application of IL-27 (100 ng/ml) elicited immediate but transient calcium spikes in just 1.03% of total mTGNs (Figure 2c), confirming that IL-27 can directly activate a small subgroup of sensory neurons.

To further examine the effect of IL-27 on sensory neurons, we treated cultured mTGNs with media ± IL-27 (100 ng/ml, 6 hours) and analyzed transcripts by RT-qPCR. IL-27 treatment did not influence *F2rl1* (Figure 2d) or *Mrgprc11* (Figure 2e); however, it increased the transcription of *Bst1* (Figure 2f) and *Stat1* (Figure 2g). BST2, also known as CD317/tetherin, has an unidentified function in itch. Given the regulatory role of Jak in IL-27 signal transduction (Kalliolias and

Ivashkiv, 2008), we investigated their involvement in IL-27–induced BST2 transcription. Cultured mTGNs were pretreated with a Jak inhibitor (100 nM) or vehicle for 1 hour, followed by stimulation with IL-27 (100 ng/ml) or vehicle for 6 hours. RT-qPCR was employed to examine the mRNA levels of *Stat1* and *Bst2*. The Jak inhibitor effectively reduced IL-27–induced *Stat1* transcription levels but had no impact on *Bst2* transcription levels (Figure 2h). Thus, STAT1 may not mediate IL-27/BST2 signaling in sensory neurons.

To investigate the possible BST2 release induced by IL-27, we performed ELISA on the culture supernatant of mTGNs after treatment with IL-27 (100 ng/ml, 24 hours). Compared with vehicle, IL-27 induced a significant release of BST2 (Figure 2i). To investigate whether BST2 could act as a direct or indirect itch inducer in healthy skin, we utilized the murine cheek injection model of acute itch. Mice received intradermal injections of either vehicle (saline, 4 µl) or BST2 (1 µg, 4 µl) into the right cheek, and bouts of site-directed hind limb scratches were recorded (30 minutes). In this study, BST2 injection promoted a significant increase in average scratching bouts relative to vehicle treatment (Figure 2j). Examination of the temporal profile showed that BST2-induced scratching bouts peaked in significance at 10 minutes, whereas the highest average was at 15 minutes (Figure 2k). In contrast, BST2 injection did not promote pain-like, wiping behaviour (data not shown). Thus, IL-27 directly activates a subpopulation of sensory neurons and promotes the BST2 pathway that induces itch response. These findings suggest that IL-27 signals through distinct itch pathways in sensory neurons and keratinocytes, involving the activation of BST2 and PAR2, respectively.

BST2 expression is increased in human lesional AD skin and murine AD-like models, colocating with sensory nerve endings, highlighting its connection to sensory neurons

Our findings demonstrate a link between IL-27 signaling and BST2 expression in cultured sensory neurons. However, the relevance of BST2 signaling in human pruritic skin conditions remained unknown. To further examine an association of BST2 expression with disease activity, we performed RNA-sequencing analysis on lesional AD (LAD), nonlesional AD, and healthy control (HC) skin samples. This revealed a significant upregulated BST2 transcription in LAD in comparison with that in HC (Figure 3a). Importantly, the BST2 upregulation is not present in nonlesional AD, which is also demonstrated by Fragments Per Kilobase of transcript per Million mapped reads (Figure 3a).

To validate the regulation of BST2 expression in pruritic lesions on protein level, we performed immunohistochemical staining of human HC and LAD skin. In HC skin, BST2 immunosignals were predominantly observed in the dermis, with minimal presence in the epidermis. However, in LAD, these BST2 signals were elevated in the dermis and at the dermal–epidermal junction, surpassing the levels seen in HC (Figure 3b), which is consistent with the RNA-sequencing result (Figure 3a). In this study, the pattern of BST2

and n ≥ 6 mice per group for in vivo studies); N.S.: $P > .05$, $*P < .05$, $**P < .01$, and $***P < .001$, with Student *t*-test. AUC, area under the curve; h, hour; i.d., intradermal; N.S., not significant; PAR2, protease-activated receptor 2; phKC, primary human keratinocyte; s, second; Veh, vehicle.

ARTICLE IN PRESS

Y Li et al.
Neuronal BST2: Pruritic Mediator in IL-27−Driven Itch
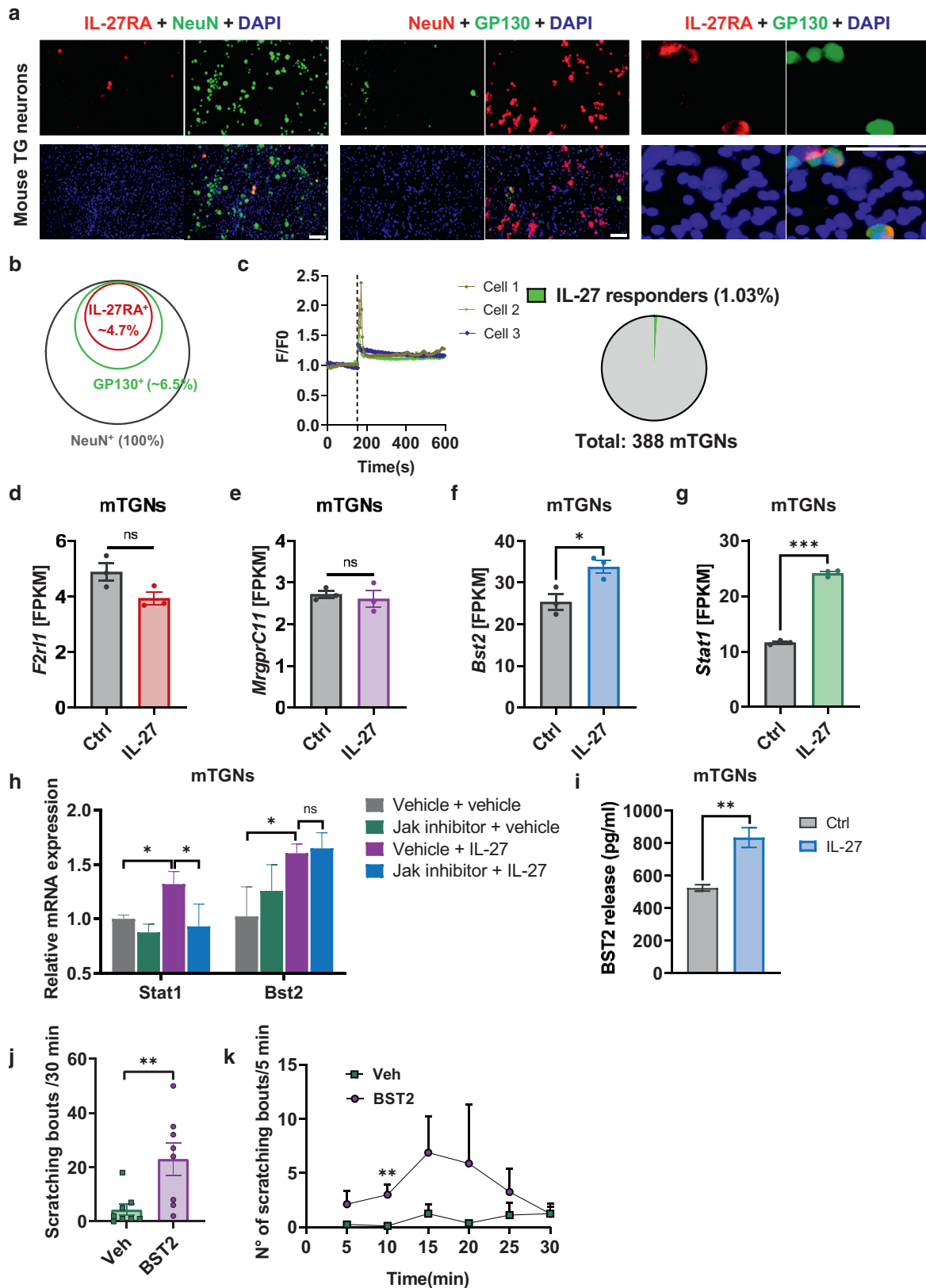
Figure 2. IL-27 activates sensory neurons, leading to the upregulation of *Bst2* transcripts; BST2 elicits acute itch response in mice. (a) Images of cultured mTGNs showing expression of IL-27RA and NeuN and GP130 and NeuN and magnified image showing colocalization of IL-27RA and GP130 (right). Bars = 100 μm. (b) Diagram indicating the percentage of IL-27RA+ and GP130+ cells within the NeuN+ mTGN. (c) Calcium mobilization in cultured mTGNs after IL-27 application (added at the dotted line), with graph depicting calcium traces and Venn diagram indicating percentage. (d, e) RNA-seq of the FPKM of (d) *F2rl1*, (e) *Mrgprc11*, (f) *Bst2*, (g) *Stat1* transcription in cultured mTGNs induced by IL-27. (h) mTGNs were pretreated with a Jak1 inhibitor or vehicle for 1 h before mTGNs were stimulated with IL-27 or vehicle for 6 h. Gene transcription levels of *Stat1* and *Bst2* were examined by RT-qPCR. (i) ELISA for BST2 release

Figure 3. BST2 is upregulated in human skin with lesional AD; BST2 resides near the sensory nerve endings in skin samples from human and murine lesional AD. (**a**) RNA-seq analysis of LAD and NLAD skin with data expressed as $\log_2$FCH relative to HCs (left) and the average RPKM value obtained for each disease condition (right). (**b**) Representative immunostaining of human HC and LAD skin showing the distribution pattern of BST2 (green), PGP9.5 (red), and DAPI (blue), with an enlarged graph showing fluorescence intensity at a focused area with punctate PGP9.5 staining. Bars = 50 µm. (**c**) Representative immunostaining of ear skin from EtOH- and MC903-treated mice showing the expression of BST2 (green), PGP9.5 (red), and DAPI (blue). Bars = 50 µm (for left) and 5 µm (for right). For **a**, data represent *FDR < 0.05 and [ns]FDR > 0.05. n = 5 donors per group. AD, atopic dermatitis; EtOH, ethanol; FCH, fold change; FDR, false discovery rate; HC, healthy control; LAD, lesional atopic dermatitis; NLAD, nonlesional atopic dermatitis; ns, not significant; PGP9.5, protein gene product 9.5; RNA-seq, RNA sequencing; RPKM, Reads per Kilobase Per Million mapped read.
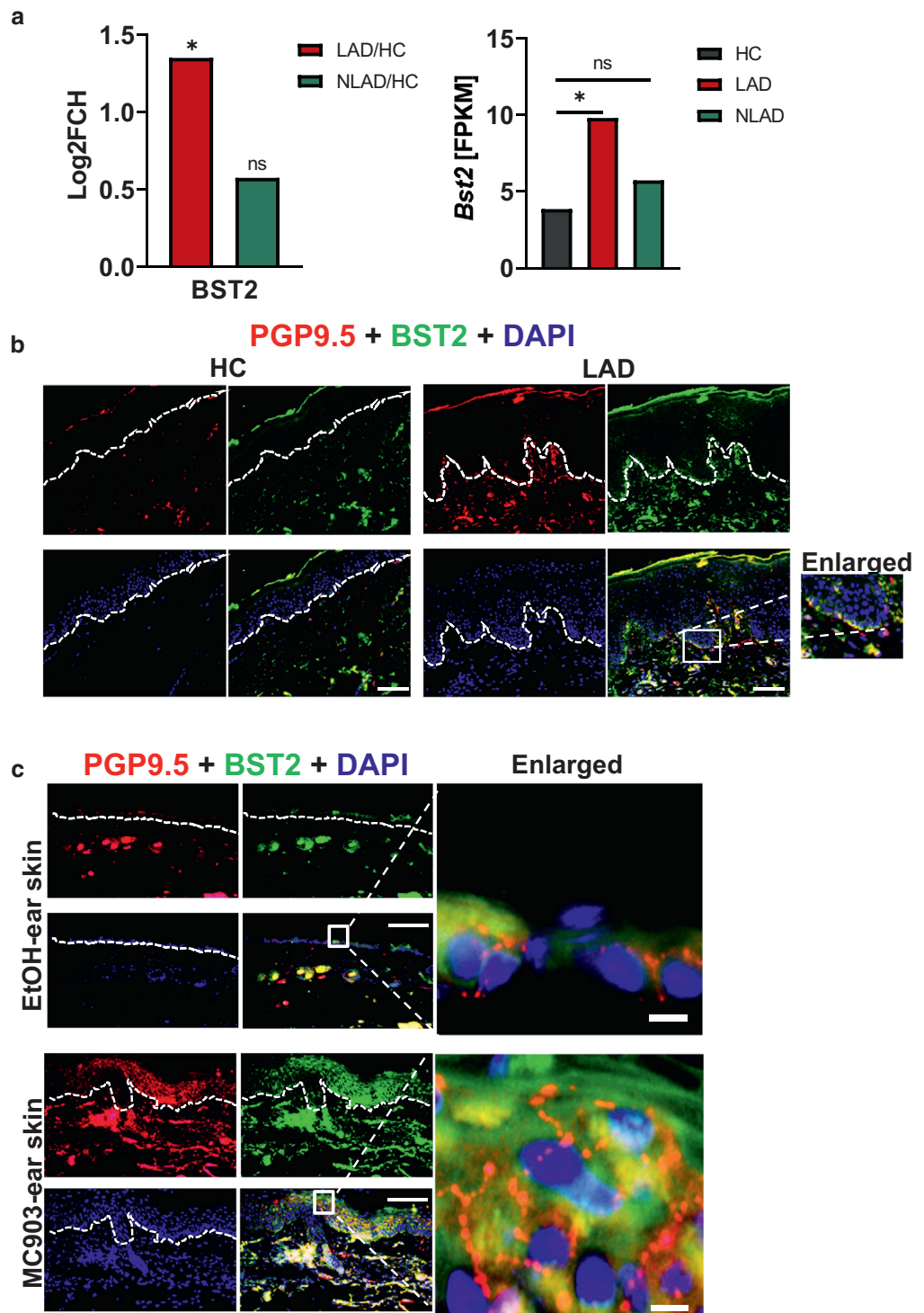
expression was additionally observed on a more detailed level with the colabeling with protein gene product 9.5, a neuronal marker. Interestingly a striking colocalization expression of BST2/protein gene product 9.5 in LAD skin was revealed when compared with that in HC skin (Figure 3b, enlarged). These findings suggest a notable correlation between BST2 expression and lesional atopic skin, likely associated predominantly with sensory nerves.

ARTICLE IN PRESS

Y Li et al.
Neuronal BST2: Pruritic Mediator in IL-27—Driven Itch

To confirm BST2 association with sensory nerve endings in murine dermatitis skin, topical MC903-treated mice were investigated, which represent a commonly used prolonged itch model and display many of the clinical features of AD, including pruritic, erythematous plaques and papules (Walsh et al, 2019). In this study, on day 9 of modeling, ear skin samples from vehicle- and MC903-treated mice were probed with antibodies targeting BST2 and protein gene product 9.5. BST2 expression was upregulated in the lesional skin of MC903-treated ears (Figure 3c). In resemblance to its expression in human skin (Figure 3b), BST2 immunosignal was evidently elevated in the lesional epidermis of MC903-treated mice compared with that in control (ethanol-treated mice) (Figure 3c). A similar trend is evident in both dermal and epidermal layers of MC903-induced lesions, with treated samples showing a striking increase in BST2 and protein gene product 9.5 colocalization relative to that in ethanol-treated skin (Figure 3c, enlarged). This finding highlights a possible link between BST2 and sensory neurons; however, whether this contributes to skin itch requires further investigation.

IL-27 receptors are overexpressed in human LAD skin, and IL-27 activates keratinocytes and induces transcription and release of BST2 and other potent pruritic and inflammatory mediators

To further understand the differential contribution of IL-27 signaling in regulation of itch sensation through BST2, the expression of the IL-27 receptors, IL-27RA and GP130, in LAD and HC skin was evaluated. Immunohistochemistry revealed a striking increase of *IL27RA* and *GP130* mRNA expression in the epidermis of LAD skin compared with that in HC skin (Figure 4a). This observation was confirmed at the single cell level, with IL-27RA and GP130 expression being markedly stronger in keratinocytes from LAD skin than in keratinocytes from HC skin (Figure 4b). Interestingly, GP130-specific immunosignal is found in all epidermal layers except in the basal layer, whereas IL-27RA is expressed throughout the epidermis of LAD and HC skin (Figure 4a). These findings suggest that disease-related regulation of IL-27 receptors occurs in keratinocytes in AD.

Subsequently, examination of IL-27RA and GP130 expression in cultured phKCs using fluorescent immunocytochemistry revealed that 6.9% of the total phKCs were IL-27RA/GP130 double positive and 19.34% single positive for GP130 (Figure 4c). The higher proportion of GP130+ cells might be due to GP130 acting as a common receptor subunit for all members of the IL-6 family of cytokines (Jones et al, 2018). To confirm the functional expression of the IL-27 receptor heterodimer in phKCs, we conducted calcium mobilization assays. Application of IL-27 (100 ng/ml) indeed led to an increase in intercellular calcium in a subset of phKCs (5.84% of total cells), suggesting functional IL-27 receptor expression (Figure 4d). Interestingly, the number of IL-27—responsive phKCs approximately matched the percentage of IL-27RA+ phKCs detected by immunofluorescence analysis (6.9%) (Figure 4c).

To examine the impact of IL-27 on keratinocyte transcription and function, we subjected mRNA of IL27-challenged (100 ng/ml, 6 hours) and vehicle-challenged phKCs to RNA sequencing. IL-27 treatment enhanced the transcription of a wide variety of signaling proteins, including *CXCL9*, *CXCL11*, *ICAM1*, *IL-32*, *IL-6*, *IL-7*, *IL-15*, *AIM2*, transcription regulatory *IRF1*, *CX3CL1*, *IFIT3*, *CSF1*, matrix metalloproteinase 3, matrix metalloproteinase 25, *TNFSF10*, and *GBP1* (Figure 4e). Moreover, IL-27 increased the transcription of itch-related genes, including *CXCL10*, *CCL2*, *IL15*, toll-like receptor 3 gene *TLR3*, *IL7R*, and *IL13RA2* (Figure 4e), and cell structural genes, including *FLT3LG*, *SPP1*, and *IFI30* (Figure 4e). Among these, CXCL9 and CXCL10 are two mediators that have previously been linked to downstream IL-27 signaling (Shibata et al, 2010).

Of the IL-27—induced transcripts detailed earlier, IL-27 treatment also significantly increased *BST2* transcripts in phKCs (Figure 4e, red bar). Subanalysis identifying the average Fragments Per Kilobase of transcript per Million mapped reads confirmed a marked upregulation of *BST2* over multiple readings by IL-27 in phKCs (Figure 4f), indicating that BST2 might be of importance in AD. Subsequently, a time-dependent analysis of IL-27—induced effect by RT-qPCR demonstrated that the IL-27—mediated regulation of BST2 transcripts in phKCs appeared to be time dependent and progressing between 2 and 36 hours of IL-27 stimulation (100 ng/ml) (Figure 4g). Moreover, the possible release of BST2 was analyzed in phKCs after incubation with IL-27 (100 ng/ml). Contrary to the readily release of BST2 observed in sensory neurons (c.f. Figure 2g), BST2 was only detected in the cell lysate (Figure 4h) rather than in cell culture supernatant (data not shown).

Mice with specific knockout of BST2 in sensory neurons displayed reduced itch responses to topical MC903, whereas depletion of BST2 in keratinocytes did not affect MC903 itch

To provide a clearcut investigation on the role of BST2 in itch, mice with depletion of BST2 specifically in sensory neurons and keratinocytes were generated after crossing BST2$^{flox/flox}$ with Avil-Cre or K14-Cre mice (Figure 5a). Sensory neuron—specific gene Advillin (Avil)$^+$/Cre-knockin (ie, Avil-Cre) mice are commonly employed to discern the functions of neuronal proteins in the sensory neuronal systems from others (Zurborg et al, 2011). A portion of exon 1 of *BST2* gene, encoding the translational start, was excised from the conditional mutant strain (Figure 5a). Two mouse lines were obtained, named Avil-Cre;Bst2$^{fl/fl}$ or K14-Cre;Bst2$^{fl/fl}$, in which BST2 is specifically knocked out in sensory neurons or keratinocytes, respectively (Figure 5b). After genotyping, Avil-Cre;Bst2$^{fl/fl}$ and K14-Cre;Bst2$^{fl/fl}$ mice exhibited normal growth rate, survival, and phenotype, compared with the BST2$^{fl/fl}$ control littermates and age-matched wild-type mice, thus suitable for evaluating their behavior characteristics (Figure 5c). Fluorescent immunohistochemistry revealed the specific depletion of BST2 protein from the tissue sections of trigeminal ganglionic neurons of Avil-Cre;Bst2$^{fl/fl}$ mice and skin keratinocyte layer of K14-Cre;Bst2$^{fl/fl}$ mice compared with those of control mice (Figure 5d)

To analyze the response to itch, MC903 model was established on the cheek of Avil-Cre;Bst2$^{fl/fl}$ and K14-Cre;Bst2$^{fl/fl}$ mice, and the results were compared with those of BST2$^{fl/fl}$ littermate control. Topical application of MC903 or ethanol was performed on the cheek daily for up to 8 days. Behavior scoring demonstrated that there was a significant

Y Li et al.
Neuronal BST2: Pruritic Mediator in IL-27–Driven Itch
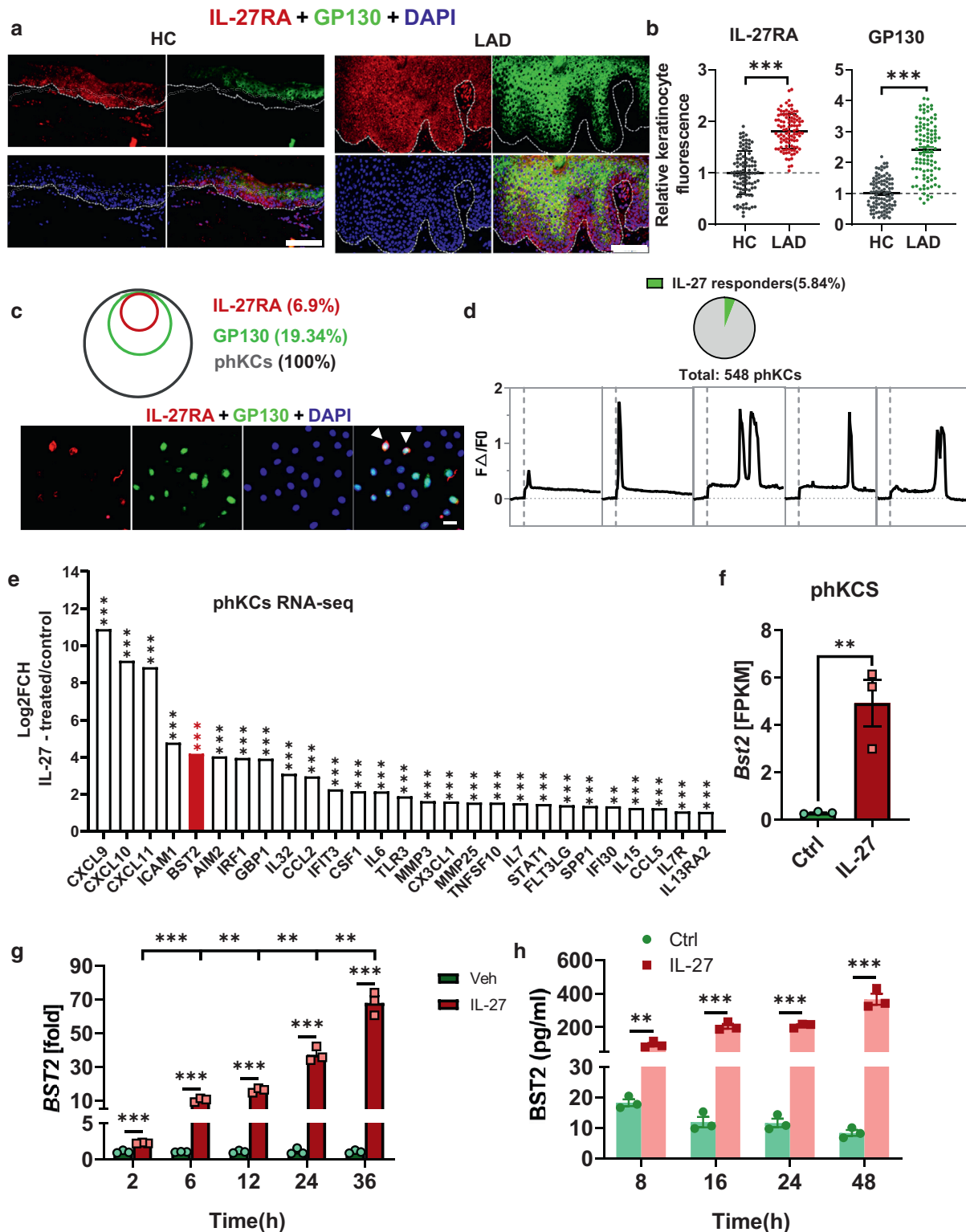
Figure 4. IL-27 receptors are overexpressed in human LAD; IL-27 activates keratinocytes, inducing transcription of BST2 and other pruritic and inflammatory mediators. (**a**) Representative images of human HC and LAD skin showing expression of IL-27RA, GP130, and DAPI and (**b**) comparison of fluorescence intensity at individual keratinocyte levels. Bars = 100 μm. (**c**) Representative immunostaining of cultured phKCs showing expression of IL-27RA, GP130, and DAPI, with a diagram indicating the percentage of IL-27RA$^+$ and GP130$^+$ phKCs. Bars = 20 μm. (**d**) Calcium mobilization in phKCs after IL-27 application (added at dotted line) and chart indicating IL-27–responsive subpopulation. (**e, f**) Effect of IL-27 (6 h) on gene transcription in phKCs: (**e**) RNA-seq and (**f**) BST2 (FPKM). (**g, h**) Effect of IL-27 on *BST2* (**g**) gene transcription and (**h**) cellular content over time in phKCs. Data represent mean ± SEM (n ≥ 3). For **e**, ***FDR < 0.001, **0.001 < FDR < 0.01, and ^{ns}FDR > 0.05. For others, N.S.: $P > .05$, **$P < .01$, and ***$P < .001$, with Student t-test. CTRL, control; FDR, false discovery rate; FPKM, Fragments Per Kilobase of transcript per Million mapped read; h, hour; HC, healthy control; LAD, lesional atopic dermatitis; N.S., not significant; phKC, primary human keratinocyte; RNA-seq, RNA sequencing; Veh, vehicle.
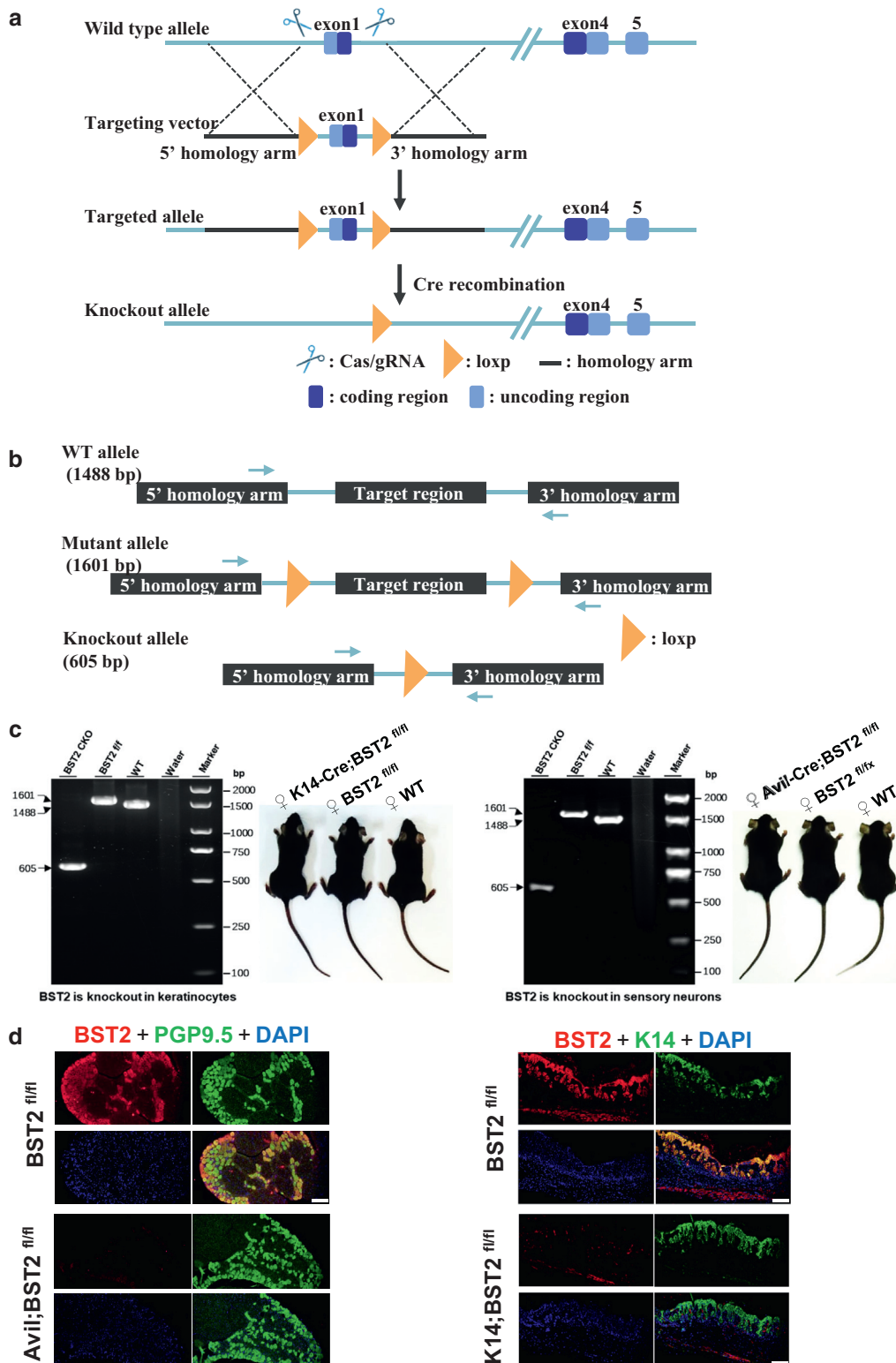
Figure 5. Generation and characterization of sensory neuron− and skin-selective BST2-KO mice, named Avil (or K14)-Cre;Bst2$^{fl/fl}$ mice, by crossing BST2$^{flox/flox}$ mice with Avil (or K14)-Cre mice. (**a**) Schematic representation of targeting the deletion of exon 1 through cre-lox system of conditional gene deletion. (**b**) Genotypic strategy and (**c**) PCR analysis as well as phenotype of CKO mice, compared with that of BST2$^{flox/flox}$ and WT mice. Genotyping confirmed the presence of the correct size of KO alleles. Both the Avil-Cre;Bst2$^{fl/fl}$ and K14-Cre;Bst2$^{fl/fl}$ mice were viable, appeared normal, and did not exhibit any noticeable phenotypic alternation up to adulthood compared with control littermates and age-matched WT mice. (**d**) Representative immunofluorescence imaging for BST2 plus PGP9.5 on the trigeminal ganglia section from Avil-Cre;Bst2$^{fl/fl}$ compared with that from BST2$^{fl/fl}$ littermate control mice (left) and BST2 plus K14 on the skin section from K14-Cre;Bst2$^{fl/fl}$ compared with that from BST2$^{fl/fl}$ littermate control mice (right). Bars = 100 μm. Avil, advillin; CKO, conditional knockout; K14, keratin 14; KO, knockout; PGP9.5, protein gene product 9.5; WT, wild type.

ARTICLE IN PRESS

Y Li et al.
Neuronal BST2: Pruritic Mediator in IL-27—Driven Itch

Figure 6. Selectively knockout of BST2 in sensory neurons attenuated MC903-induced prolonged itch; however, knockout of BST2 in keratinocytes did not demonstrate significant effect. (**a**) Comparison of MC903-induced itch-like behavior in Avil-Cre;Bst2$^{fl/fl}$ with that in BST2$^{fl/fl}$ littermate control mice. (**b**) Comparison of MC903-induced itch-like behavior in K14-Cre;Bst2$^{fl/fl}$ compared with that in BST2$^{fl/fl}$ littermate control mice. For **a** and **b**, data represent mean ± SEM; n ≥ 8 per group; N.S.: $P > .05$, $*P < .05$, $**P < .01$, and $***P < .001$, with Student t-test. (**c**) Comparison of the immune cell infiltration labeled by antibodies against CD11b, Mcpt8, and CD68 in MC903 skin from Avil-Cre;Bst2$^{fl/fl}$ versus that from BST2$^{fl/fl}$ littermate mice. In the bar chart, 3 mice per group were analyzed, and 3 images were captured from each mouse. Bars = 50 µm. $*P < .05$, $**P < .01$, and $***P < .001$, with Student t-test. K14, keratin 14; min, minute; N°, number; N.S., not significant.
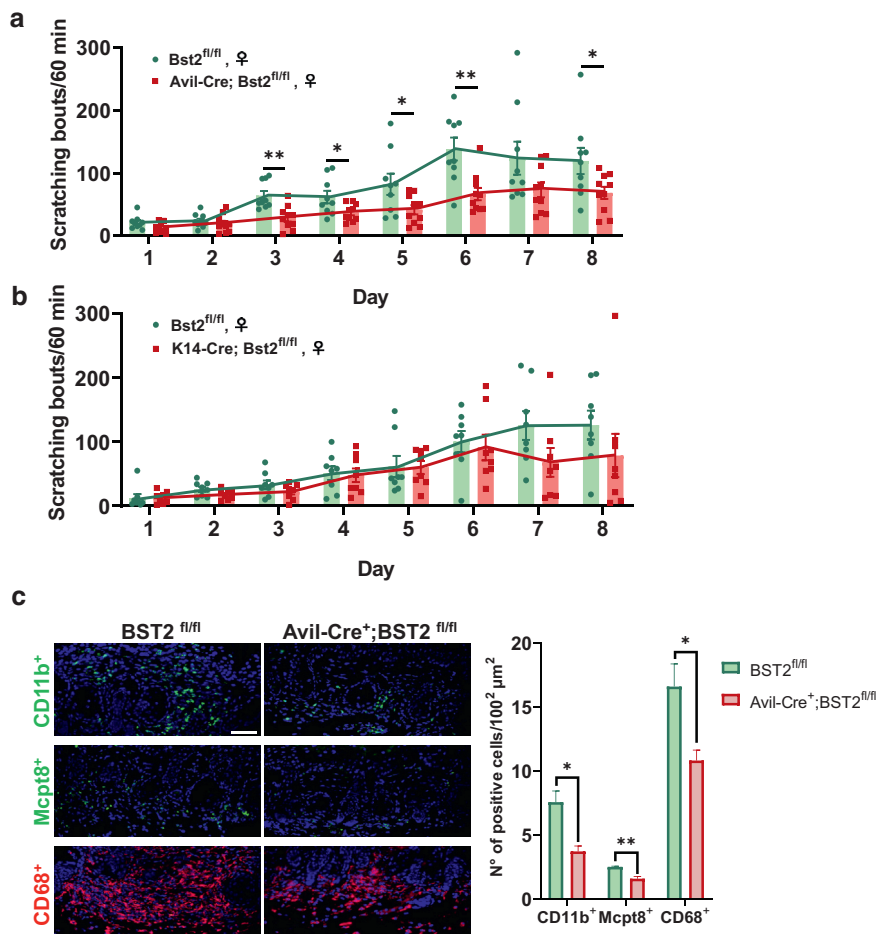
reduction in MC903-induced scratching bouts in Avil-Cre;Bst2$^{fl/fl}$ mice compared with that in BST2$^{fl/fl}$ littermate mice at days 3—8 (Figure 6a), confirming the requirement of sensory neuronal BST2 in MC903-induced pruritus. In great contrast, no reduction was seen in scratching bouts in K14-Cre;Bst2$^{fl/fl}$ mice compared with that in BST2$^{fl/fl}$ littermate mice up to 8 days (Figure 6b), confirming that sensory neuron—derived BST2 is indispensable for MC903-induced pruritus. An additional study was then focused on the skin pathological changes in the MC903-treated Avil-Cre;Bst2$^{fl/fl}$ mice compared with that in BST2$^{fl/fl}$ littermate mice. Immunohistochemical analysis of the MC903 skin revealed a significantly lower number of immune cells labeled with antibodies against CD68, CD11b, and Mcpt8 in Avil-Cre;Bst2$^{fl/fl}$ mice compared with that in BST2$^{fl/fl}$ littermate mice (Figure 6c), suggesting reduced immune cell infiltrations in the inflamed skin when the function of BST2 in sensory neurons is impaired.

To assess whether cutaneous BST2 could directly activate epidermal keratinocytes, we also measured the effect of BST2 on calcium fluctuations in cultured phKCs. At all tested concentrations, BST2 increased intercellular calcium in a subpopulation of phKCs, acting directly and dose dependently on epidermal keratinocytes (Supplementary Figure S1a). In addition, we treated cultured phKCs with media ± BST2 (250 ng/ml, 24 hours) and analyzed transcripts by RNA sequencing. BST2 treatment enhanced the transcription of several signaling proteins, namely *SLURP1*, *SPINK7*, *ARG1*, *S100A7*, and *USP2* (Supplementary Figure S1b). Among these upregulated transcripts, *SLURP1* and *SPINK7* are known to be upregulated in AD (Dežman et al, 2017; Weber et al, 2017). Furthermore, after 24-hour incubation, BST2 enhanced the release of IL-5, myeloperoxidase, kallikrein 3, VEGF, CXCL11, pentraxin 3, IFN-γ, and matrix metalloproteinase 9 from phKCs (Supplementary Figure S1c). Myeloperoxidase and matrix metalloproteinase 9 contribute to neutrophil recruitment and activation, potentiating skin irritation in AD (Li et al, 2017; Trush et al, 1994). CXCL11 is a potent T-cell chemoattractant and a biomarker of chronic AD lesions (Mansouri and Guttman-Yassky, 2015; Oetjen and Kim, 2018). IFN-γ is also associated with chronic AD lesions, impairing epidermal barrier function and driving both subacute and chronic inflammation (Kanoh et al, 2019; Ospelnikova et al, 2017). In addition, we stimulated an immortalized human keratinocyte cell line (HaCaT) with media ± BST2 (250 ng/ml, 8 minutes) and analyzed cellular lysate using a phosphokinase array. BST2 promoted phosphorylation and activation of a wide range of phosphokinases, including several STATs, Src-family kinases, and a number of inflammation-related transcription factors (Supplementary Figure S1d). Thus, BST2 represents a potent driver of cutaneous inflammatory cascades, activating

ARTICLE IN PRESS

Y Li et al.
Neuronal BST2: Pruritic Mediator in IL-27—Driven Itch

epidermal keratinocytes and promoting dermatitis-linked inflammation.

DISCUSSION

IL-27 is a pleiotropic mediator with dual functionality, acting as both a proinflammatory and anti-inflammatory cytokine, which results in highly divergent and, at times, opposing functions within the immune system. Although previous reports have highlighted IL-27 overexpression in chronic lesional allergic eczematous skin, as opposed to the acute phase of eczema (Wittmann et al, 2009), the exact role of IL-27 in AD has remained enigmatic. Our recent findings provide compelling evidence of IL-27 signaling playing a significant role at the periphery in pruritic AD skin conditions.

In this study, we observed a significant upregulation of IL-27 and its receptors in lesional AD skin, underscoring the relevance of this pathway in AD pathology. The IL-27 receptors, IL-27RA and GP130, were found to be upregulated in lesional AD skin, strengthening the connection between IL-27 signaling and chronic inflammation. Cheek (intradermal) injection of IL-27 failed to induce acute itch—like responses in mice, suggesting its limited pruritogenic potential as a direct itch inducer. We observed that IL-27 may indirectly promote itch sensation through the modulation of PAR2, a critical receptor for allergen responsiveness, skin lesion formation, and neuroepidermal communication in AD and itch (Braz et al, 2021; Buhl et al, 2020). In our study, IL-27 enhanced the transcription of PAR2 (*F2RL1*) and sensitized SLIGRL-induced calcium responses and increased PAR2-mediated itch in mice. In this regard, keratinocyte-specific overexpression of PAR2 results in AD-like lesions characterized by epidermal hyperplasia, ichthyosis, and itching (Frateschi et al, 2011). PAR2-overexpressed mice also display exaggerated allergen-induced responses, with application of house dust mites evoking severe itch-like responses, triggering inflammatory skin lesions, and enhancing brain natriuretic peptide transcription in adjacent sensory neurons (Meng et al, 2018). In addition, PAR2 mediates TRPV3 signaling in keratinocytes, which induces itch directly and indirectly through pruritogens, including TSLP (Zhao et al, 2020) and Serpin E1 (Larkin et al, 2021), and orchestrate the immune response toward a Th2 phenotype. Notably, SLIGRL-induced itch predominantly has been reported to rely on keratinocyte PAR2 because MRGPRC11 does not exist in these cells (Liu et al, 2011). In our assay, neither MRGPRC11 nor PAR2 in sensory neurons displayed upregulation in response to IL-27. This further excludes the possibility of SLIGRL-induced itch being influenced by sensory inputs. Thus, these findings shed light on a previously unrecognized IL-27/PAR2 signaling pathway in skin-derived itch and confirm that IL-27 is capable of modulating purinoreceptors to enhance itch signaling.

PAR2 activation has been shown to induce TSLP transcription in keratinocytes (Moniaga et al, 2013; Ziegler et al, 2013). In the skin that received intradermal IL-27 + SLIGRL injection, TSLP levels were enhanced compared with those of SLIGRL alone. Notably, IL-27 alone also increased TSLP transcription. Similarly, the skin injected with trypsin, a known PAR family activator, exhibited a significant increase in TSLP levels. Moreover, coinjection of IL-27 and trypsin produced enhanced scratching behaviors compared with trypsin alone. Although coinjection of IL-27 with trypsin showed an elevated TSLP level, albeit not significant, this may not be solely attributed to IL-27's effect on PAR2 because IL-27 alone induces TSLP transcription. This finding suggests a potential involvement of TSLP in the pathogenesis of IL-27—induced itch.

A surprising finding is the discovery of a previously unreported downstream effector of IL-27, BST2, because BST2 was traditionally characterized as a type II transmembrane protein, which when tethered to the plasma membrane can restrict the release of enveloped viruses. BST2 has also been linked to exosomes and has been detected in the plasma of patients with colorectal carcinoma (Chiang et al, 2015). Tumor tissue is capable of releasing BST2 into the circulatory system where it stimulates cell-to-cell interaction and adhesion (Mahauad-Fernandez and Okeoma, 2015). Although BST2 reduces measles virus release from nonneuronal cells, knockout of BST2 did not reduce the survival rate of measles virus—challenged mice, suggesting its antiviral effects to be specific to certain cell types or viruses. Previous reports also demonstrated that in primary monocytes and T cells, IL-27 enhanced BST2 expression (Guzzo et al, 2012); however, this seemed to be related to the antiviral action of IL-27/BST2 (Bego et al, 2015; Chiang et al, 2015).

In our findings, BST2 exhibited overexpression in lesional dermatoses, primarily localized closely to sensory nerve endings in both human and atopic murine models, with comparatively lower expression levels in the epidermis. These findings indicate the association of BST2 with AD disease condition. In this context, the skin of mice with dermatitis challenged with oxazolone has revealed an upregulation in *Bst2* transcripts (Ewald et al, 2017). Although both neuronal and non-neuronal BST2 can function as antiviral protein in restricting viral spread in the body, diversity in the biological function of BST2 has been revealed (Holmgren et al, 2015; Presle et al, 2021; Xu et al, 2021). Neuronal BST2 is associated with functions related to neuronal development, synaptic plasticity, and potentially neuroimmune interactions. Non-neuronal BST2 may contribute to immunomodulation responses, cytokinesis, and cell adhesion mechanisms, among other functions. Thus, cell-type—specific regulation of BST2 associated with various diseases might result in the distinct role of BST2 in dermatophysiological aspects in sensory neurons and keratinocytes.

In this study, our data have provided additional insights into the distinct roles of BST2 in itch sensation within sensory neurons and keratinocytes. IL-27 exerts control over the synthesis and release of BST2 in sensory neurons despite a small fraction of neurons expressing IL-27 receptors and responding to IL-27 application in vitro. However, IL-27 does not stimulate BST2 release in keratinocytes, despite their established role as a BST2 source, and IL-27 continues to govern both the synthesis dose dependently and the intracellular content of BST2 in keratinocytes. These findings highlight the differential function of BST2 in distinct cell types. Whether BST2 functions as a soluble exosome-dependent mediator or plasma membrane—tethered protein on keratinocytes or both, with property known to be

associated with non-neuronal cells, is unclear. Different isoforms of BST2 due to post-transcriptional regulation may vary between normal and cancer states (Mahauad-Fernandez and Okeoma, 2015). If this indeed leads to cell-specific functional differences in pruritus, it underscores the need for future investigations in this area. Notably, atopic skin exhibited heightened BST2 expression in immunofluorescent staining, with notable immunoreactivity closely associated with sensory nerve endings. Importantly, tissue-specific knockout of sensory neuronal BST2 resulted in an alleviated MC903-induced prolonged itch, whereas no such effect was observed upon BST2 knockout in keratinocytes, highlighting the pivotal role of neuronal BST2 in itch pathogenesis. These newly generated transgenic mice exhibited no discernible abnormal phenotypes compared with their control littermates and age-matched wild-type mice. Consequently, it appears that BST2 is not essential for maintaining normal physiological functions in sensory neurons and keratinocytes. It is likely that this disparity of BST2 in itch signaling may be attributed to the regulatory mechanism in the availability of extracellular BST2 release. However, the intriguing question remains whether the extracellular BST2 available in the cutaneous vicinity reaches a physiological concentration sufficient to induce itch sensations.

Furthermore, we have demonstrated that intradermal cheek injection of BST2 induces acute itch—like behaviors in mice, with a rapid and significant response observed within the first 5—10 minutes after injection. These findings suggest its potential role as a pruritogen in mice. This aligns with the hypothesis that extracellular BST2 may contribute to itch sensation. In addition, we observed that the application of either IL-27 or BST2 to keratinocytes resulted in the upregulation of cytokines, chemokines, and pruritogens, ultimately leading to a dermatitis-like phenotype. Specifically, BST2 directly activated a significant population of keratinocytes, resulting in dose-dependent calcium influx, upregulated transcripts linked to itch and inflammation, and activated an array of intracellular kinases, thus inducing dermatitis-associated phenotype. It seems unlikely that ILT7 contributes to itch on sensory neurons because it is absent from mTGNs on the basis of our transcriptomic analysis. However, the exact mechanism of BST2 in the interaction with keratinocytes remained to be further defined. A previous report from plasmacytoid dendritic cells revealed that BST2 can bind to ILT7 (encoded by *LILRA4*), activating plasmacytoid dendritic cells and modulating nucleic acid—induced inflammation (Bego et al, 2015; Cao et al, 2009). Furthermore, activation of ILT7 results in Src/Syk-dependent calcium fluctuations in plasmacytoid dendritic cells (Cao et al, 2006). Although ILT7 is generally reported as a plasmacytoid dendritic cell—specific receptor, it has been found to be upregulated in pooled skin samples from pruritic LAD skin, relative to that in healthy skin (*LILRA4*) (fold change of reads per kilobase per million mapped reads = 3.88) (Nattkemper et al, 2018). Thus, it remains to be investigated whether the BST2-induced responses in the skin could be mediated by ILT7, with ILT7 facilitating cellular activation and meditating enhanced itch transduction in pruritic conditions.

In this study, we have identified BST2 as a potential pruritogen, which may be linked, at least partially, to

IL-27—associated pruritus. This neuroepidermal IL-27/BST2 and skin IL-27/PAR2 as well as IL-27/TSLP pathways that are centered by IL-27 facilitate interconnection between immune cells, keratinocytes, and sensory neurons, likely playing a role in lesional pruritus and may contribute to the pathological itch/scratch cycle. Our data strongly support the therapeutic potential of targeting the IL-27 pathway in the management of inflammatory skin diseases characterized by neuroimmune interactions and pruritus, offering a promising avenue for addressing chronic itch conditions.

MATERIALS AND METHODS
Human rights
The human skin tissues were purchased from Tissue Solutions (Glasgow, Scotland); thus, institutional approval and patient consent were not necessary.

Animals
All animal procedures were performed in accordance with the Guidelines for Care and Use of Laboratory Animals of Henan University and approved by the Animal Ethics Committee of Henan University.

The Bst2-floxed mice and Avil-Cre—transgenic mice were generated by Shanghai Model Organisms Center (Shanghai, China) using CRISPR/Cas9 gene editing and homologous recombination strategies; BST2$^{fl/fl}$ mice were crossed with Avil-Cre mice to generate the Avil-Cre;BST2$^{fl/fl}$ mice in which BST2 is deleted in peripheral sensory neurons. K14-Cre—transgenic mice were generated by Cyagen Biosciences (Suzhou, China) and crossed with BST2$^{fl/fl}$ mice to generate epithelial keratinocyte—specific conditional knockout mice (K14-Cre;BST2$^{fl/fl}$ mice). BST2$^{fl/fl}$ littermate mice were used as controls. All experiments were done with mice aged 6—8 weeks.

Antibodies, cells, and reagents for tissue culture and others are detailed in Supplementary Materials and Methods.

ORCIDs
Yanqing Li: http://orcid.org/0000-0002-4406-7878
Weiwei Chen: http://orcid.org/0000-0002-1965-7606
Xingyun Zhu: http://orcid.org/0009-0004-3368-6755
Huiyuan Mei: http://orcid.org/0009-0007-4653-4867
Jinhai Wang: http://orcid.org/0009-0007-8065-2701
Martin Steinhoff: http://orcid.org/0000-0002-7090-2187
Joerg Buddenkotte: http://orcid.org/0000-0002-2394-3269
Wenhao Zhang: http://orcid.org/0000-0003-2797-1125
Zhenghui Li: http://orcid.org/0000-0002-4796-0098
Xiaolong Dai: https://orcid.org/0000-0002-6478-5252
Chunxu Shan: http://orcid.org/0000-0001-8670-0208
Jiafu Wang: http://orcid.org/0000-0002-3654-4400
Jianghui Meng : http://orcid.org/0000-0002-3107-4200

CONFLICT OF INTEREST
MS has performed consultancy services for which he received compensation from Pfizer, Sanofi, Regeneron, Lilly, Novartis, Galderma, Leo, Merck, Avon, Pierre-Fabre, L'Oreal, BMS, Maruho, Toray, Mitsubishi, Maruho, Kiniksa,

ARTICLE IN PRESS

Y Li et al.
Neuronal BST2: Pruritic Mediator in IL-27–Driven Itch

SUPPLEMENTARY MATERIAL
Supplementary material is linked to the online version of the paper at www.jidonline.org, and at https://doi.org/10.1016/j.jid.2024.01.025.

REFERENCES
Bego MG. Côté É, Aschman N, Mercier J, Weissenhorn W, Cohen ÉA. Vpu exploits the cross-talk between BST2 and the ILT7 receptor to suppress anti-HIV-1 responses by plasmacytoid dendritic cells. PLoS Pathog 2015;11: e1005024.

Braz JM, Dembo T, Charruyer A, Ghadially R, Fassett MS, Basbaum AI. Genetic priming of sensory neurons in mice that overexpress PAR2 enhances allergen responsiveness. Proc Natl Acad Sci USA 2021;118:e2021386118.

Brown D, Trowsdale J, Allen R. The LILR family: modulators of innate and adaptive immune pathways in health and disease. Tissue Antigens 2004;64: 215–25.

Buhl T, Ikoma A, Kempkes C, Cevikbas F, Sulk M, Buddenkotte J, et al. Protease-activated Receptor-2 regulates neuro-epidermal communication in atopic dermatitis. Front Immunol 2020;11:1740.

Cao W, Bover L, Cho M, Wen X, Hanabuchi S, Bao M, et al. Regulation of TLR7/9 responses in plasmacytoid dendritic cells by BST2 and ILT7 receptor interaction. J Exp Med 2009;206:1603–14.

Cao W, Rosen DB, Ito T, Bover L, Bao M, Watanabe G, et al. Plasmacytoid dendritic cell-specific receptor ILT7-Fc epsilonRI gamma inhibits toll-like receptor-induced interferon production. J Exp Med 2006;203:1399–405.

Cevikbas F, Wang X, Akiyama T, Kempkes C, Savinko T, Antal A, et al. A sensory neuron-expressed IL-31 receptor mediates T helper cell-dependent itch: involvement of TRPV1 and TRPA1. J Allergy Clin Immunol 2014;133:448–60.

Chiang SF, Kan CY, Hsiao YC, Tang R, Hsieh LL, Chiang JM, et al. Bone marrow stromal antigen 2 is a novel plasma biomarker and prognosticator for colorectal carcinoma: A secretome-based verification study. Dis Markers 2015;2015:874054.

Cocks TM, Moffatt JD. Protease-activated receptors: sentries for inflammation? Trends Pharmacol Sci 2000;21:103–8.

Datsi A, Steinhoff M, Ahmad F, Alam M, Buddenkotte J. Interleukin-31: the "itchy" cytokine in inflammation and therapy. Allergy 2021;76:2982–97.

Dežman K, Korošec P, Rupnik H, Rijavec M. SPINK5 is associated with early-onset and CHI3L1 with late-onset atopic dermatitis. Int J Immunogenet 2017;44:212–8.

Dillon SR, Sprecher C, Hammond A, Bilsborough J, Rosenfeld-Franklin M, Presnell SR, et al. Interleukin 31, a cytokine produced by activated T cells, induces dermatitis in mice. Nat Immunol 2004;5:752–60 [published correction appears in Nat Immunol 2005;6:114].

Ewald DA, Noda S, Oliva M, Litman T, Nakajima S, Li X, et al. Major differences between human atopic dermatitis and murine models, as determined by using global transcriptomic profiling. J Allergy Clin Immunol 2017;139:562–71.

Frateschi S, Camerer E, Crisante G, Rieser S, Membrez M, Charles RP, et al. PAR2 absence completely rescues inflammation and ichthyosis caused by altered CAP1/Prss8 expression in mouse skin. Nat Commun 2011;2:161.

Guzzo C, Jung M, Graveline A, Banfield BW, Gee K. IL-27 increases BST-2 expression in human monocytes and T cells independently of type I IFN. Sci Rep 2012;2:974.

Holmgren AM, Miller KD, Cavanaugh SE, Rall GF. Bst2/tetherin is induced in neurons by type I interferon and viral infection but is dispensable for protection against neurotropic viral challenge. J Virol 2015;89: 11011–8.

Hunter CA, Kastelein R. Interleukin-27: balancing protective and pathological immunity. Immunity 2012;37:960–9.

Jones GW, Hill DG, Cardus A, Jones SA. IL-27: a double agent in the IL-6 family. Clin Exp Immunol 2018;193:37–46.

Kalliolias GD, Ivashkiv LB. IL-27 activates human monocytes via STAT1 and suppresses IL-10 production but the inflammatory functions of IL-27 are abrogated by TLRs and p38. J Immunol 2008;180:6325–33.

Kanoh H, Ishitsuka A, Fujine E, Matsuhaba S, Nakamura M, Ito H, et al. IFN-gamma reduces epidermal barrier function by affecting fatty acid composition of ceramide in a mouse atopic dermatitis model. J Immunol Res 2019;2019:3030268.

Larkin C, Chen W, Szabó IL, Shan C, Dajnoki Z, Szegedi A, et al. Novel insights into the TRPV3-mediated itch in atopic dermatitis. J Allergy Clin Immunol 2021;147:1110–4.e5.

Li C, Maillet I, Mackowiak C, Viala C, Di Padova F, Li M, et al. Experimental atopic dermatitis depends on IL-33R signaling via MyD88 in dendritic cells. Cell Death Dis 2017;8:e2735.

Liu Q, Weng HJ, Patel KN, Tang Z, Bai H, Steinhoff M, et al. The distinct roles of two GPCRs, MrgprC11 and PAR2, in itch and hyperalgesia. Sci Signal 2011;4:ra45.

Mahauad-Fernandez WD, DeMali KA, Olivier AK, Okeoma CM. Bone marrow stromal antigen 2 expressed in cancer cells promotes mammary tumor growth and metastasis. Breast Cancer Res 2014;16:493.

Mahauad-Fernandez WD, Okeoma CM. The role of BST-2/Tetherin in host protection and disease manifestation. Immun Inflamm Dis 2015;4: 4–23.

Mansouri Y, Guttman-Yassky E. Immune pathways in atopic dermatitis, and definition of biomarkers through broad and targeted therapeutics. J Clin Med 2015;4:858–73.

Meng J, Li Y, Fischer MJM, Steinhoff M, Chen W, Wang J. Th2 modulation of transient receptor potential channels: an unmet therapeutic intervention for atopic dermatitis. Front Immunol 2021;12:696784.

Meng J, Moriyama M, Feld M, Buddenkotte J, Buhl T, Szöllösi A, et al. New mechanism underlying IL-31–induced atopic dermatitis. J Allergy Clin Immunol 2018;141:1677–89.e8.

Moniaga CS, Jeong SK, Egawa G, Nakajima S, Hara-Chikuma M, Jeon JE, et al. Protease activity enhances production of thymic stromal lymphopoietin and basophil accumulation in flaky tail mice. Am J Pathol 2013;182: 841–51.

Müller SI, Friedl A, Aschenbrenner I, Esser-von Bieren J, Zacharias M, Devergne O, et al. A folding switch regulates interleukin 27 biogenesis and secretion of its alpha-subunit as a cytokine. Proc Natl Acad Sci USA 2019;116:1585–90.

Nattkemper LA, Tey HL, Valdes-Rodriguez R, Lee H, Mollanazar NK, Albornoz C, et al. The genetics of chronic itch: gene expression in the skin of patients with atopic dermatitis and psoriasis with severe itch. J Invest Dermatol 2018;138:1311–7.

Oetjen LK, Kim BS. Interactions of the immune and sensory nervous systems in atopy. FEBS J 2018;285:3138–51.

Ospelnikova TP, Genorkyan OV, Mironova TV, Andreeva SA, Kolodyazhnaya LV, Ershov FI. Features of interferon and cytokine status in atopic dermatitis. Archives of asthma, allergy and immunology 2017;1: 009–14.

Pflanz S, Hibbert L, Mattson J, Rosales R, Vaisberg E, Bazan JF, et al. WSX-1 and glycoprotein 130 constitute a signal-transducing receptor for IL-27. J Immunol 2004;172:2225–31.

Presle A, Frémont S, Salles A, Commere PH, Sassoon N, Berlioz-Torrent C, et al. The viral restriction factor tetherin/BST2 tethers cytokinetic midbody remnants to the cell surface. Curr Biol 2021;31:2203–13.e5.

ARTICLE IN PRESS

Y Li et al.
Neuronal BST2: Pruritic Mediator in IL-27—Driven Itch

Shibata S, Tada Y, Kanda N, Nashiro K, Kamata M, Karakawa M, et al. Possible roles of IL-27 in the pathogenesis of psoriasis. J Invest Dermatol 2010;130:1034—9.

Steinhoff M, Ahmad F, Pandey A, Datsi A, AlHammadi A, Al-Khawaga S, et al. Neuroimmune communication regulating pruritus in atopic dermatitis. J Allergy Clin Immunol 2022;149:1875—98.

Steinhoff M, Neisius U, Ikoma A, Fartasch M, Heyer G, Skov PS, et al. Proteinase-activated receptor-2 mediates itch: a novel pathway for pruritus in human skin. J Neurosci 2003;23:6176—80.

Steinhoff M, Schmelz M, Szabó IL, Oaklander AL. Clinical presentation, management, and pathophysiology of neuropathic itch. Lancet Neurol 2018;17:709—20.

Steinhoff M, Vergnolle N, Young SH, Tognetto M, Amadesi S, Ennes HS, et al. Agonists of proteinase-activated receptor 2 induce inflammation by a neurogenic mechanism. Nat Med 2000;6:151—8.

Sutaria N, Adawi W, Goldberg R, Roh YS, Choi J, Kwatra SG. Itch: pathogenesis and treatment. J Am Acad Dermatol 2022;86:17—34.

Tiwari R, de la Torre JC, McGavern DB, Nayak D. Beyond tethering the viral particles: immunomodulatory functions of tetherin (BST-2). DNA Cell Biol 2019;38:1170—7.

Trier AM, Kim BS. Cytokine modulation of atopic itch. Curr Opin Immunol 2018;54:7—12.

Trush MA, Egner PA, Kensler TW. Myeloperoxidase as a biomarker of skin irritation and inflammation. Food Chem Toxicol 1994;32:143—7.

Walsh CM, Hill RZ, Schwendinger-Schreck J, Deguine J, Brock EC, Kucirek N, et al. Neutrophils promote CXCR3-dependent itch in the development of atopic dermatitis. ELife 2019;8:e48448.

Wang F, Kim BS. Itch: a paradigm of neuroimmune crosstalk. Immunity 2020;52:753—66.

Weber C, Fischer J, Redelfs L, Rademacher F, Harder J, Weidinger S, et al. The serine protease inhibitor of Kazal-type 7 (SPINK7) is expressed in human skin. Arch Dermatol Res 2017;309:767—71.

Wilson SR, Thé L, Batia LM, Beattie K, Katibah GE, McClain SP, et al. The epithelial cell-derived atopic dermatitis cytokine TSLP activates neurons to induce itch. Cell 2013;155:285—95.

Wittmann M, Doble R, Bachmann M, Pfeilschifter J, Werfel T, Mühl H. IL-27 Regulates IL-18 binding protein in skin resident cells. PLoS One 2012;7:e38751.

Wittmann M, Zeitvogel J, Wang D, Werfel T. IL-27 is expressed in chronic human eczematous skin lesions and stimulates human keratinocytes. J Allergy Clin Immunol 2009;124:81—9.

Xu X, Zhang J, Li S, Al-Nusaif M, Zhou Q, Chen S, et al. Bone marrow stromal cell antigen 2: Is a potential neuroinflammation biomarker of SOD1^{G93A} mouse model of amyotrophic lateral sclerosis in pre-symptomatic stage. Front Neurosci 2021;15:788730.

Yoshimoto T, Yoshimoto T, Yasuda K, Mizuguchi J, Nakanishi K. IL-27 suppresses Th2 cell development and Th2 cytokines production from polarized Th2 cells: a novel therapeutic way for Th2-mediated allergic inflammation. J Immunol 2007;179:4415—23 [published correction appears in J Immunol 2010;184:3298].

Zhao J, Munanairi A, Liu XY, Zhang J, Hu L, Hu M, et al. PAR2 mediates itch via TRPV3 signaling in keratinocytes. J Invest Dermatol 2020;140:1524—32.

Ziegler SF, Roan F, Bell BD, Stoklasek TA, Kitajima M, Han H. The biology of thymic stromal lymphopoietin (TSLP). Adv Pharmacol 2013;66:129—55.

Zurborg S, Piszczek A, Martínez C, Hublitz P, Al Banchaabouchi MA, Moreira P, et al. Generation and characterization of an Advillin-Cre driver mouse line. Mol Pain 2011;7:66.

ARTICLE IN PRESS

Y Li et al.
Neuronal BST2: Pruritic Mediator in IL-27—Driven Itch

SUPPLEMENTARY MATERIALS AND METHODS

Animals

All animal procedures were performed in accordance with the Guidelines for Care and Use of Laboratory Animals of Henan University and approved by the Animal Ethics Committee of Henan University.

The Bst2-floxed mice and Avil-Cre—transgenic mice were generated by Shanghai Model Organisms Center (Shanghai, China) using CRISPR/Cas9 gene editing and homologous recombination strategies; BST2$^{fl/fl}$ mice were crossed with Avil-Cre mice to generate the Avil-Cre;BST2$^{fl/fl}$ mice in which BST2 is deleted in peripheral sensory neurons. K14-Cre—transgenic mice were generated by Cyagen Biosciences (Suzhou, China) and crossed with BST2$^{fl/fl}$ mice to generate epithelial keratinocytes—specific conditional-knockout mice (K14-Cre;BST2$^{fl/fl}$ mice). BST2$^{fl/fl}$ littermate mice were used as controls. All experiments were performed with mice aged 6—8 weeks.

Human samples

Human skin samples for RNA sequencing were detailed in our previous publication (Larkin et al, 2021) and reanalyzed in this study. Briefly, punch biopsies were dissected from lesional atopic dermatitis (LAD) and non-LAD areas of the skin in patients with atopic dermatitis and normal skin from healthy controls. All donors in this study were aged >17 years. LAD samples were donated by patients with atopic dermatitis with SCORing Atopic Dermatitis values >35 (n = 5). Samples were also taken from non-LAD (n = 5) skin. This human study received institutional approval from the Medical Research Council, National Scientific and Ethical Committee (Budapest, Hungary) (ETT TUKEB, document identifications: 50935/2012/EKU and 54256-1/2016/EKU). All donors provided written informed consent, in accordance with the Declaration of Helsinki principles.

Human skin biopsies for immunohistochemistry were purchased from Tissue Solutions (Glasgow, United Kingdom). These paraffin-embedded samples were donated by either patients or healthy individuals.

Culturing and stimulation of primary human keratinocytes

Primary human keratinocytes (phKCs) were seeded into 24-well plates and cultured in KBM-Gold medium with KBM Gold SingleQuot keratinocyte supplement (Lonza, Basel, Switzerland). Cells were incubated in the medium for 3 days before performing any experiments.

Prior to signaling assays, phKCs were incubated with hydrocortisone-free medium for ≥24 hours. For signaling assays, phKCs were stimulated with media ± IL-27 (100 ng/ml, 24 hours, 2526-IL-010/CF, R&D System) or BST2 (250 ng/ml, 24 hours, 9939-BS, R&D System), and cell-culture supernatants were collected, pooled, and analyzed by cytokine array. Moreover, cultured phKCs were also treated with media ± IL-27 (100 ng/ml, 6 hours or various time points), and gene transcription was measured using RNA sequencing (RNA-seq) or qPCR.

Culturing and stimulation of primary sensory neurons

Mouse trigeminal neurons (mTGNs) were isolated from postnatal C57BL/6 mice. Mice received an intraperitoneal injection (0.2% xylazine, 1% ketamine, 0.9%

intraperitoneal), resulting in deep anesthetization. Harvested ganglia were incubated with a dissociation solution containing collagenase I (10 mg/ml, Sigma-Aldrich) and dispase II (5 mg/ml, Sigma-Aldrich) in PBS salt solution for 30 minutes. Digests were then washed with DMEM, and cell suspension was filtered through a 100-µm cell strainer. Cells were seeded into precoated 24-well plates (poly-L-lysine [Sigma-Aldrich], laminin [Sigma-Aldrich]) and cultured for 7 days as described previously (Meng et al, 2018). Culture medium consisted of DMEM (D6429, Sigma-Aldrich) supplemented with fetal bovine serum (5% [v/v], F8687, Sigma-Aldrich), penicillin (100 U/ml, Gibco), streptomycin (100 µg/ml, Gibco), cytosine β-d-arabinofuranoside (10 µM, Sigma-Aldrich), B27 (Gibco), and nerve GF (50 ng/ml, Sigma-Aldrich).

For signaling assays, mTGNs were incubated with IL-27 (100 ng/ml, 24 hours, 2799-ML-010/CF, R&D System), BST2 (500 ng/ml, 24 hours, 9940-BS, R&D System), or the appropriate vehicle control (24 hours). Cell-culture supernatants were collected and analyzed by cytokine array. Cultured mTGNs were also treated with media ± IL-27 (100 ng/ml, 6 hours) or BST2 (500 ng/ml, 6 hours) or pretreated with Jak inhibitor (100 nM, 1 hour, T3080, TargetMol), and gene transcription was measured using RNA-seq.

Cytokine array

Cell-culture supernatants from phKCs were collected, pooled, and analyzed using Proteome Profiler Human XL Cytokine Array Kit (ARY022B, R&D System) according to the manufacturer's instructions. Cell-culture supernatants from mTGNs were collected and analyzed using the Proteome Profiler Mouse Cytokine Array Kit, panel A (ARY006, R&D System) according to the manufacturer's instructions. Cytokine spots were quantified using ImageJ software (National Institutes of Health, Bethesda, MD). Densitometry values were calculated, and treated samples were expressed as the fold change relative to nontreated controls.

qPCR

After treatment, phKCs and mTGNs were processed for qPCR. BST2 and protease-activated receptor 2 cDNA expression levels were measured using SYBR Green ROX mix (ABI) and real-time fluorescence. A total of 1 µg of RNA samples were reverse transcribed into cDNA using the high-capacity cDNA reverse transcription Kit (catalog number 4368814, Thermo Fisher Scientific) following the manufacturer's instruction. qPCR was performed by incubating cDNAs with the SYBR Green PCR Master mix (catalog number 4309155, Thermo Fisher Scientific) and normalized to GAPDH levels. Primers were bought from OriGene or synthesized by Sangon Biotech (Shanghai, China)—human BST2 forward: TCTCCTGCAACAAGAGCTGACC; human BST2 reverse: TCTCTGCATCCAGGGAAGCCAT; human protease-activated receptor 2 forward: CTCCTCTCTG TCATCTGGTTCC; and human protease-activated receptor 2 reverse: TGCACACTGAGGCAGGTCATGA.

RNA-seq

RNA-seq of human skin samples was performed by IMGM Laboratories (Planegg, Germany), which has been reported in our previous publication (Larkin et al, 2021). Total RNA was

ARTICLE IN PRESS

Y Li et al.
Neuronal BST2: Pruritic Mediator in IL-27–Driven Itch

prepared from human skin biopsies (detailed earlier) with the RNeasy Fibrous Tissue Mini Kit (Qiagen) followed by on-column DNase digestion. Samples were analyzed using the 2100 Bioanalyzer (Agilent Technologies) and RNA 6000 Nano/Pico LabChip Kits (Agilent Technologies). Library was prepared using the TruSeq Stranded mRNA HT technology. The pooled sequencing library was quantified using the highly sensitive fluorescent dye–based Qubit ds DNA HS Assay Kit (Invitrogen). Sequencing of the library was performed on the NextSeq 500 sequencing system (Illumina) and was operated under the control of the NextSeq Control Software. Primary image processing was performed on the NextSeq 500 instrument using Real Time Analysis 2.4.11 Software. Primary data analysis was performed using the bcl2fastq 2.15.04 software package. The Illumina Sequence Analysis Viewer 2.4.5 was used for imaging and evaluation of the sequencing run performance. The CLC Genomics Workbench 11.0.1 (CLC bio, a Qiagen company) was used for in-depth analysis of differentially expressed genes. BST2 levels in diseased skin (LAD, non-LAD) were filtered from our previous dataset reported in Larkin et al (2021) and then expressed relative to healthy controls and graphed as average $\log_2$ fold change.

RNA-seq of phKCs and mTGNs was performed by the Beijing Genomics Institute (Shenzhen, China). Briefly, total RNA was extracted from the cells using Trizol (Invitrogen, Carlsbad, CA). Oligo (dT)-attached magnetic beads were used to purify mRNA before the latter was fragmented into small pieces with fragment buffer. First-strand cDNA was generated using random hexamer-primed reverse transcription, followed by a second-strand cDNA synthesis. A-Tailing Mix and RNA Index Adapters were added by incubating to end repair. The cDNA fragments obtained from the previous step were amplified by PCR, and products were purified by Ampure XP Beads and then dissolved in EB solution. The final library was amplified with phi29 to make a DNA nanoball, which had >300 copies of 1 molecule. DNA nanoballs were loaded into the patterned nanoarray, and single-end 50-base reads were generated on a DNBseq platform. First quality control of sequencing data (raw reads/raw data) was performed to determine eligibility for subsequent analysis: sequencing data filtering was performed using SOAPnuke software developed by Beijing Genomics Institute. The filtered clean reads were aligned to the reference sequence. Quantitative gene analysis and analyses based on gene expression (principal component, correlation, differential gene screening, etc) were conducted, and resultant RNA-seq original data have been deposited to Gene Expression Omnibus (accession number GSE188242) (National Center for Biotechnology Information tracking system number 22499629).

A fold change of 2 or greater (ie, $\log_2$ fold change ≥ 1) was considered significant in each RNA-seq comparison. False discovery rates (FDRs) were determined and classified as ***FDR < 0.001, **0.001 < FDR < 0.01, *0.01 < FDR < 0.05, and [ns]FDR > 0.05.

Intracellular calcium measurement
Cultured phKCs or mTGNs were loaded with Fluo-4 AM (3 μM, 30 minutes, 37 °C). Cells were then washed, and while being imaged, cells were stimulated with IL-27 (100 ng/ml, R&D System), BST2 (100–500 ng/ml, R&D System), SLIGRL (10 μM, Sigma-Aldrich) or LIGRLS (10 μM, Sigma-Aldrich), or vehicle controls. Images were captured at 4-second intervals using MateXpress 6 software by ImageXpress Micro 4 Automated Cell Imaging System (Molecular Devices). For mTGNs, intracellular calcium increases were normalized to F/F0, with F denoting the fluorescence and F0 denoting the baseline fluorescence, and graphed relative to time. Responding cells were analyzed and presented as percentage total neurons. For phKCs, intracellular calcium increases were normalized to FΔ/F0, with FΔ denoting the change of stimulated fluorescence over the baseline fluorescence (F0), and graphed relative to time. Only cells demonstrating a 30% increase over baseline were considered responsive (FΔ/F0 ≥ 0.3). Responding cells were also examined with respect to their maximum intensity of fluorescence ($(FΔ/F0)_{max}$) and the time point at which maximum fluorescence was achieved ($Time_{max}$) (Larkin et al, 2021).

ELISA
Cell-culture supernatants from mTGNs were detected by the BST2 ELISA Kit (abx388698, Abbexa). mTGNs were treated with IL-27 (100 ng/ml) or vehicle for 24 hours. The supernatants were collected and centrifuged at 1000*g* for 20 minutes at 4 °C before being used for ELISA analysis, according to the manufacturer's instructions.

Cell lysates from phKCs were detected by human BST2 ELISA kit (ab231931, Abcam). phKCs were treated with IL-27 (100 ng/ml) or vehicle for 8, 16, 24, and 48 hours. We removed growth media and rinsed adherent cells 3 times in PBS, solubilized the cells with the addition of 750 μl chilled Cell Extraction Buffer, scraped the cells into a microfuge tube, incubated the lysate on ice for 15 minutes, and centrifuged at 18,000*g* for 20 minutes at 4 °C before the supernatants were used for ELISA analysis, according to the manufacturer's instructions.

Quantitative analysis was performed on a microplate reader (Infinite M plex, Tecan). For each experiment, 3 replicates were used for analysis.

Cheek injection model of acute itch
C57BL/6 female mice (aged 6–8 weeks, originally sourced from SPF Biotechnology, Beijing, China) received intradermal injections of BST2 (1 μg, 4 μl, R&D System) or vehicle control (saline, 4 μl) into the right cheek. The resulting behavioral responses were recorded for 30 minutes. Bouts of hind limb scratches, directed to the injection site, were considered indicative of pruritus (Kido-Nakahara et al, 2014; LaMotte et al, 2011). Wiping was considered indicative of pain.

MC903-treated mouse model of atopic dermatitis
The MC903-induced atopic dermatitis–like mouse model was performed as described previously (Larkin et al, 2021). C57BL/6 female mice (aged 6–8 weeks, originally sourced from SPF Biotechnology) were treated daily; a topical solution of MC903 (4 nmol, 20 μl in ethanol, Sigma-Aldrich) or vehicle (ethanol, 20 μl) was applied to the left and right ear or the cheek (for transgenic mice studies), respectively. On day 9, mice were killed, and ears were collected, processed, and embedded in paraffin for immunohistochemical analysis.

ARTICLE IN PRESS

Y Li et al.
Neuronal BST2: Pruritic Mediator in IL-27−Driven Itch

Culturing and stimulation of a keratinocyte cell line (HaCaT) and phosphokinase array

The immortalized human keratinocytes (HaCaT) from adult donors were obtained from iCell (iCell-h066, iCell Bioscience). Cells were maintained at 37 °C, with 5% carbon dioxide in a humidified environment with DMEM (D6429, Sigma-Aldrich) plus 10% fetal bovine serum (F8687, Sigma-Aldrich) and penicillin−streptomycin (15140122, Gibco) on T75 flasks. Before performing experiments, cells were serum starved for 4 hours before preincubated with 250 ng/ml BST2 for 8 minutes. Cell lysate was harvested for kinase array (ARY003B, R&D System) in accordance with the manufacturer's instructions. After enhanced chemiluminescence development, the lanes were analyzed using the G BOX gel documentation system.

Acute cheek itch model

To analyze the influence of protease-activated receptor 2 activation on IL-27−induced itch-like behavior, C57 BL/6 mice were intradermally injected with IL-27 (400 ng,10 µl), SLIGRL (40 nmol, 10 µl), trypsin (100 µg, 10 µl, T1426, Sigma-Aldrich), or their combination into the right cheek. Control mice were given Tyrode's solution (137 mM sodium chloride, 2.7 mM potassium chloride, 1.0 mM magnesium chloride, 1.8 mM calcium chloride, 20 mM 4-[2-hydroxyethyl]-1-piperazineethanesulfonic acid, 5.6 mM glucose, pH 7.4; 10 µl). All the mice were video recorded for 30 minutes for the analysis of scratching bouts.

Immunohistochemistry

Paraffin sections of human and mouse skin were deparaffinized, rehydrated, permeabilized (Triton X-100 [0.2%], PBS), and incubated in blocking solution (normal donkey serum [5%], PBS) for 1 hour. Specimens were then incubated (4 °C, overnight) with blocking solution containing primary antibodies targeting IL27RA (ab5996, Abcam, 1:200), GP130 (MAB4681, R&D System, 1:100), GP130 (ab21864, Abcam, 1:200), NeuN (ab177487, Abcam, 1:3000), RBFOX3/NeuN (NBP1-92693SS, Novus Biologicals, 1:400), BST2 (ab88523, Abcam, 1:150), and BST2 (DDX0390P-100, Novus Biologicals, 1:100). Specimens were washed (PBS) and incubated with anti-mouse (Alexa 488, donkey) and/or anti-rabbit (Alexa 594, donkey). After washing (PBS), specimens were mounted using prolong anti-fade reagents containing DAPI (Thermo Fisher Scientific). Images were taken by a Leica DMi8 confocal microscope equipped with LASX software or an IX73 Olympus inverted microscope with CellSens Dimension Imaging software. Relative cell fluorescence was analyzed using ImageJ and calculated to allow for comparison of protein expression at the single keratinocyte level.

Data analysis

Data are presented as mean ± SEM using Prism (GraphPad Software, La Jolla, CA). We made 2-group comparisons with a 2-tailed Student's t-test, followed by Welch's correction; $P < .05$ is considered significant. To analyze the itch-like behavior, data are presented as means ± SEMs (n ≥ 8 mice per group), *$P < .05$, **$P < .01$, and ***$P < .001$, with Student's t-test. To determine the difference in frequencies of responders in calcium transient measurements, chi-square statistic test was applied: https://www.socscistatistics.com/tests/chisquare/default2.aspx. For RNA-seq, the average fold change for genes upregulated was plotted. Differentially expressed genes are defined on the basis of the following thresholds: $\log_2$ fold change ≥ 1.0 and the adjusted P-value FDR < 0.05. FDRs were indicated as ***FDR < 0.001, **0.001 < FDR < 0.01, *0.01 < FDR < 0.05, and ^{ns}FDR > 0.05. For genes not reaching these thresholds, although FDR < 0.05, these are not defined as differentially expressed genes.

SUPPLEMENTARY REFERENCES

Kido-Nakahara M, Buddenkotte J, Kempkes C, Ikoma A, Cevikbas F, Akiyama T, et al. Neural peptidase endothelin-converting enzyme 1 regulates endothelin 1-induced pruritus. J Clin Invest 2014;124:2683−95.

LaMotte RH, Shimada SG, Sikand P. Mouse models of acute, chemical itch and pain in humans. Exp Dermatol 2011;20:778−82.

Larkin C, Chen W, Szabó IL, Shan C, Dajnoki Z, Szegedi A, et al. Novel insights into the TRPV3-mediated itch in atopic dermatitis. J Allergy Clin Immunol 2021;147:1110−4.e5.

Meng J, Moriyama M, Feld M, Buddenkotte J, Buhl T, Szöllösi A, et al. New mechanism underlying IL-31-induced atopic dermatitis. J Allergy Clin Immunol 2018;141:1677−89.e8.

Supplementary Figure S1. BST2 directly activates keratinocytes, upregulates itch-related transcripts, and triggers potent inflammatory cascades. (**a**) Calcium mobilization in cultured phKCs after BST2 application (various concentrations [100, 200, and 500 ng/ml]; added at the dotted line), with graphs depicting response profiles and charts indicating the percentage of BST2-responsive cells. Each red dot represents a BST2-responsive phKC graphed with respect to its $(F\Delta/F0)_{max}$ and $time_{max}$ values. (**b, c**) Effect of BST2 (250 ng/ml, 24 h) on (**b**) gene transcription and (**c**) cytokine release in cultured phKCs. (**d**) Effect of BST2 (250 ng/ml, 8-min incubation) on phosphorylated kinase activation in the HaCaT cell line. Data represent mean ± SEM (n ≥ 3). N.S.: $*P > .05$, $**P < .01$, and $***P < .001$, with Student t-test. For RNA-seq, $***FDR < 0.001$, $**0.001 < FDR < 0.01$, $*0.01 < FDR < 0.05$, and $^{ns}FDR > 0.05$. FCH, fold change; FDR, false discovery rate; h, hour; max, maximum; min, minute; N.S., non-significant; phKC, primary human keratinocyte; RNA-seq, RNA sequencing; s, second.